Model Error Resolution Document

Complete only applicable items.

INITIATION

1. Originator: Jerry McNeish	2. Date: April 16, 2008	3. ERD No. MDL-WIS-PA-000005 ERD 02

4. Document Identifier: MDL-WIS-PA-000005 REV 00; and AD 01	5. Document Title: Total System Performance Assessment Model/Analysis for the License Application

6. Description of and Justification for Change (Identify applicable CRs and TBVs):

This Error Resolution Document (ERD) is provided to update the TSPA-LA AMR Rev 00, and AD01 to correct issues identified in the following condition reports (CRs). There is no impact to the overall conclusion of the AMR caused by these minor corrections.

CR 11861—Typo in table column. The numbers (1,940 and 1,257) located in the fourth (Short canister) and fifth (Long Canister) lines of the second column, of Table 6.3.7-1, Waste Package Configurations, are reversed and should be corrected. The DIRS report for Volume I encountered no changes for this change to Table 6.3.7-1.

CR 11875—Incorrect text in Section 7.7.3. The TSPA for LA (MDL-WIS-PA-000005 Rev 00) has incorrect text in Section 7.7.3.3 and 7.7.3.11. All the modeling work that supports the text is correct. Correct text is provided in Attachment 1 to this ERD. In addition, during extent of condition review other clarification was required in Section 8, pp 8-43[a] and 8-78[a]. This information is also provided in Attachment 1.

CR 11884—Dissolved concentration uncertainty discussion error. Table P-6 on page P-35 of AMR MDL-WIS-PA-000005, Rev. 00, Section 7.2.6[a] on page 7.18[a] and Table P-6[a] on page P-18[a] of Addendum 01 contain an error in the discussion of the uncertainty of dissolved concentrations related to temperature conditions. This issue is known by the authors of the SAR and the appropriate corrective actions are being incorporated during the development of the SAR. The following updated text should replace the first full paragraph on page 7-18[a], and the fourth paragraph in Table P-6[a] on Pager P-18[a] of Addendum 01. (Note: The Rev 00 text is updated by the Addendum update to Appendix P):

The lower temperature limit for the range of applicability of the Dissolved Concentration Limits Abstraction is 25°C. Because actinides in carbonate systems, such as those that will prevail in the EBS, have retrograde solubility, abstractions for the solubility of actinides were developed for conditions at 25°C and provide bounding values for the temperature range of applicability up to 100°C, but there is no explicit temperature dependence in the abstractions for actinide solubility in the EBS (SNL 2007 [DIRS 177418], Section 6.3.3.3). The TSPA-LA Model applies the Dissolved Concentration Limits Abstraction at temperatures below 25°C. Because actinides have retrograde solubility, it is possible that dissolved concentration limits below 25°C could be slightly higher than those implemented in the TSPA-LA Model. The degree of variation has been evaluated for the actinide solubility solids modeled at temperature of 25°C and 100°C (SNL 2007 [DIRS 177418], Table 6.3-4). This temperature variation magnitude can be compared to the base-case solubility model uncertainty (these are the characteristic

CONCURRENCE

	Printed Name	Signature	Date
7. Checker	DAVID MOHR	David E Mohr	5/6/08
8. QCS/QA Reviewer	JOHN K. DEVERS	John K Devers	05/06/08
APPROVAL			
9. Originator	JERRY McNEISH	Jerry A McNeish	5.6.08
10. Responsible Manager	Paul R. Dixon	Paul R	5-6-08

INITIATION

1. Originator: Jerry McNeish	2. Date: April 16, 2008	3. ERD No. MDL-WIS-PA-000005 ERD 02
4. Document Identifier: MDL-WIS-PA-000005 REV 00; and AD 01	5. Document Title: Total System Performance Assessment Model/Analysis for the License Application	

6. Description of and Justification for Change (continued):

values related to the uncertainty in the equilibrium constants, i.e., the log K terms) that is summarized in the Dissolved Concentration Limits Abstraction (SNL 2007 [DIRS 177418], Table 8-2). That comparison shows that for the actinides, the 95% confidence limits (i.e., 2) for the model cover between about one-third to two or three times the entire range of temperature variation from 25°C to 100°C of the model (e.g., SNL 2007 [DIRS 177418], Figure 6.3-3). For small temperature variations below 25°C (i.e., decreases of about 10 degrees), variations in the dissolved concentration limits models for actinides are expected to be only a fraction of those changes from 25°C to 100°C, and therefore should be smaller than the uncertainty captured explicitly within the models. Because the Dissolved Concentration Limits Abstraction includes treatment of the major uncertainties (SNL 2007 [DIRS 177418], Section 6.3.3), it is expected that dissolved concentration limits at lower temperatures would be within the range of uncertainty captured in the Dissolved Concentration Limits Abstraction. Radium solubility is higher at higher temperatures and the abstraction developed at 100°C is conservatively applied to all temperatures below 100°C.

CR 11885—Incorrect information in Appendix K. The three scatterplots at the bottom of Figure K7.8.2-2[a] (00817DC_0882a) are repeats of the scatterplots in Figure K7.8.1-2[a] (00817DC_0885a) rather than the intended scatterplots. The figure needs to be updated with the correct scatterplots. The corrected figure (K7.8.2-2[a]) is provided in Attachment 2 to this ERD. Figure K7.8.1-2[a] is also included in Attachment 2 to correct a minor formatting error on the y-axis of scatterplot (b).

CR 11889—Typos in symbols in pdf version of Appendix J. The specialized font used for several symbols in Appendix J was inadvertently not embedded into the pdf when it was created. For example, a special S symbol became a sigma symbol. Other symbols that were altered were still recognizable (A, and E) but not as intended by the author. The affected pages are provided in Attachment 3 to this ERD.

CR 11892—Appendix K errors in variable description. The CR initially pointed to the error listed below as (1). Other corrections to the Table were identified upon further evaluation and are summarized and provided as appropriate in Attachment 4 of the ERD.

(1) **SEEPCOND**: The epistemic uncertain variable **SEEPCOND** (used in the sensitivity analyses) is incorrectly listed as **SEEPCON*** (parameter name in the table is incorrect and the asterisk indicates incorrectly that the variable is not considered in sensitivity analysis due to correlations). To correct this error, the entry in Table K3-1 needs to be replaced with the name **SEEPCOND**. Also, SEEPCON should be changed to SEEPCOND on pages TK-48, and TK-105. A reference to Section 6.3.3.2.2 and Table 6.3.3-5 is also needed in all three tables (K3-1, K3-2, K3-3).

(2) FRACCHNL: (Table K3-1) and Fraction_Channel_a (Table K3-2) lower end of range should be 0.09.

(3) KDNPCOL: The value for KDNPCOL is changed for the results reported in App K[a], from the value presented in Rev 0. The value used for dose results in the Appendix K[a] is 10 to 500, uniform distribution.

(4) RHI85: Table K3-1, K3-2, and K3-3 should refer only to Section 6.3.4.1 and to Table 6.3.4-3.

(5) WDDSAGGC: In Tables K3-1, K3-2, and K3-3, the entry for this parameter should read "Distribution: Student-t with 5 degrees of freedom. Mean: 46.1. Standard deviation 1.19." rather than "Distribution: Normal. Mean: 46.067. Standard deviation 1.187." The Student-t was implemented and is documented in the source DTN to TSPA.

Model Error Resolution Document

Complete only applicable items.

INITIATION

1. Originator: Jerry McNeish	2. Date: April 16, 2008	3. ERD No. MDL-WIS-PA-000005 ERD 02
4. Document Identifier: MDL-WIS-PA-000005 REV 00; and AD 01	5. Document Title: Total System Performance Assessment Model/Analysis for the License Application	

6. Description of and Justification for Change (continued):

Additional corrections to Appendix K[a].

Add following note to Appendix K[a]:

The Table K3-1 entry for KDNPCOL is altered for the results reported in Appendix K[a]. The *Kd* range for sorption of Np on the uranium colloids is given by a log-uniform distribution ranging from 10 to 500 mL/g (Table 6.3.7-64). The lower bound value of 10 mL/g was incorrectly set to 1 mL/g during implementation. This value was changed to the correct value of 10 mL/g in TSPA-LA Model v5.005.

CR 11899—Use of surrogate in GW protection case. The Naval Nuclear Propulsion Program (NNPP) received a comment on their Technical Support Document that the TSPA-LA is silent on the use of a surrogate to represent NNPP Spent Nuclear Fuel (SNF) for the groundwater case. This issue is known by the authors of the SAR and the appropriate corrective actions are being incorporated during the development of the SAR. The new paragraph to be inserted in the Addendum to the end of Section 7.5.3 is as follows:

The following analyses are also applicable to the groundwater protection standards at 10 CFR 63.331, which consider the 10,000-year maximum mean activity concentrations for radium (^{226}Ra and ^{228}Ra) and the alpha emitters (including ^{226}Ra but excluding radon and uranium isotopes), and the 10,000-year maximum mean annual dose for the beta and photon emitters. In particular, the activity released as a function of time for ^{226}Ra and ^{228}Ra is lower for the nominal/early failure naval SNF inventory compared to the commercial SNF inventory (Output DTN: MO0707EMPDECAY.000), as are the activities of their parent actinide isotopes (namely, ^{234}U and ^{230}Th for ^{226}Ra, and ^{236}U and ^{232}Th for ^{228}Ra). The activity released as a function of time for the alpha, beta, and photon emitters associated with the nominal/early failure naval SNF inventory are also lower when compared to the commercial SNF inventory. Since the activity curves of the radionuclides considered in the groundwater protection standard for the nominal/early failure naval SNF inventory are bounded by the commercial SNF inventory, and taking into account the structure and slower dissolution of the naval SNF, commercial SNF is an appropriate surrogate for naval SNF with respect to the groundwater protection standards.

CR 11905—Clarification of paragraph in TSPA-LA AMR. The second paragraph of Section 8.2.4.1[a] (page 8-34[a]) of AMR MDL-WIS-PA-000005 (TSPA-LA), Rev. 00, Addendum 01, needs clarification. This issue is known by the authors of the SAR and the appropriate corrective actions are being incorporated during the development of the SAR.

The following statement should replace the existing second paragraph:

The radionuclides that contribute most to the estimate of mean annual dose are presented on Figure 8.2-12[a]. The mean dose curves on Figure 8.2-12a[a] illustrate that five radionuclides, ^{99}Tc, ^{14}C, ^{129}I, ^{36}Cl, and ^{79}Se contribute the most to the maximum mean annual dose for the 10,000 year time period. Two of these species, ^{36}Cl and ^{79}Se, were not listed in the parent document as important due to an implementation error, as documented in Appendix P, Section P2, of the parent document. As can be seen from Figure 8.2-12b[a], in the post 10,000 year period the dominant radionuclides before 800,000 years are ^{99}Tc, and ^{129}I; at 1.000,000 years are ^{129}I, ^{242}Pu, and ^{237}Np. In the results presented in this addendum, ^{226}Ra is less influential due to a correction for the longitudinal dispersivity used in the SZ Flow and Transport Submodel documented in Section 6.3.10[a] and Appendix P, Section P15, of the parent document.

CR 11909—Supplemental Plots. AMR MDL-WIS-PA-000005, Rev. 00, TSPA-LA and Addendum 01 did not provide plots for data found in DTN: MO0801TSPAWPDS.000 and MO0710ADTSPAWO.000 related to the "Fraction of Drift Filled with Rubble", and the "Spatially Averaged Waste Package Outer Barrier Thicknesses for 1 Million Years for (a) Commercial SNF Waste Packages and (b) Codisposal Waste Packages." A new output DTN (MO0803TSPAPSAR.000 [DIRS 185276])

INITIATION

1. Originator: Jerry McNeish	2. Date: April 16, 2008	3. ERD No. MDL-WIS-PA-000005 ERD 02
4. Document Identifier: MDL-WIS-PA-000005 REV 00; and AD 01	5. Document Title: Total System Performance Assessment Model/Analysis for the License Application	

6. Description of and Justification for Change (continued):

provides the plots generated from the two noted DTNs. This issue is known by the authors of the SAR and the appropriate corrective actions are being incorporated during the development of the SAR. See Attachment 5 for the new figures.

CR 11912—EXDOC Mathcad comparison. Section 7.3.2.2 has the following sentence: "The EXDOC calculation of expected annual dose for the Waste Package EF Modeling Case was verified by reproducing the EXDOC results using Mathcad (output DTN: MO0708TSPAVALI.000 [DIRS 182985])". The Mathcad files mentioned were done in support of the development of the TSPA AMR, but only recently finalized and not submitted in the above mentioned DTN. These calculations have been finalized and submitted in a supplemental DTN (DTN: MO0803ADTSPASA.000 [DIRS 185302]).

CR 11915—TSPA-LA AMR references to TDIPs. TSPA AMR (MDL-WIS-PA-000005) and associated DIRs report incorrectly, listed the following TDIPs: (1) TDR-TDIP-NS-000006 [DIRS 180677]; (2) TDR-TDIP-ES-000001 [DIRS 181031]; and (3) TDR-TDIP-NS-000005 [DIRS 179412]. The non-design TDIPs in the majority of cases were replaced by references to an AMR. These three were mistakenly left in the TSPA AMR. DIRS 181031 is incorrectly listed in Section 7.4.5.4.2 and in Section 9, and 180677 and 179412 were only in Section 9, the reference list. These TDIPs should be removed from the document and the reference list. The following specific changes should be made:

Section 7.4.5.4.2, second paragraph:

> "*The uncertainty/variability characterization reviews examined the following key parameters of the DSs (SNL 2007 [DIRS 180778], Sections 6.1.5[a] through 6.1.7[a]) and WPs (SNL 2007 [DIRS 181953], Table 8-1):*"

Section 9.1: Remove the entries for 181031, 180677, and 179412.

CR 11916—Update Section 7.8 referencing. Section 7.8.2, 3rd paragraph, 4th bullet: Change as shown:

- Geochemistry—The uraninite ore at the Nopal I mine has been altered to secondary uranium minerals, such as oxyhydroxides, schoepite, and uranyl silicates, such as boltwoodite and uranophane. The SNF at Yucca Mountain will be primarily uranium oxide, which is essentially uraninite, and the fuel is also expected to be altered to schoepite and uranyl silicates (Ebert et al. 2005 [DIRS 173071], Executive Summary; BSC 2004 [DIRS 169218], Sections 4.2).

Section 7.8.2.3, 1st paragraph, 5th bullet: Change as shown:

- The regional, surface-water-discharge location for the Nopal I ore deposit is approximately 10 km from the deposit, versus an approximate 60 km to 80 km travel distance to the nearest surface-water discharge for the Yucca Mountain flow system at the Franklin Lake Playa (DOE 2000 [DIRS 155970], Section 5.3, and Appendix I, Sections I.1 and I.4.5)

CR 11921—Typo in calculation. TSPA-LA AMR Addendum p. 8-6[a] contains a calculation for the mean probability of volcanic eruptions that occur within 10,000 years. The calculation should be changed to $(0.083) \times (1.69 \times 10^{-8}) \times (10^{4}\ \text{yr}) = 1.4 \times 10^{-5}$.

CR 11922—Section 8.2,4,1[a] clarification. (See write up for 11905).

This Error Resolution Document (ERD) also provides corrections to the following errors that have been identified in the TSPA-LA AMR Rev 00, and AD01 since the release of these documents:

Section 7.3.1.1 text. The first paragraph of this section incorrectly gives the number of epistemic parameters as 300. The correct number is 305. The updated text to replace this paragraph is as follows:

Model Error Resolution Document

Complete only applicable items.

INITIATION

1. Originator: Jerry McNeish	2. Date: April 16, 2008	3. ERD No. MDL-WIS-PA-000005 ERD 02
4. Document Identifier: MDL-WIS-PA-000005 REV 00; and AD 01	5. Document Title: Total System Performance Assessment Model/Analysis for the License Application	

6. Description of and Justification for Change (continued):

As outlined in Section 6.1.3, values for epistemic parameters are selected using an LHS technique. In the TSPA-LA Model, the LHS includes 305 epistemic uncertain parameters in the groundwater model (comprising all modeling cases except the Volcanic Eruption Modeling Case) and 87 epistemic uncertain parameters in the model for the Volcanic Eruption Modeling Case. The parameters are listed in Table K.3-1. Section 7.4 describes review efforts undertaken to ensure that uncertainty in important parameters is appropriately characterized. The base sample size for the LHS is 300 for all modeling cases.

Tables K3-1, K3-2, and K3-3. This number of epistemically uncertain parameters includes six BDCFs that were left out of the tables in Appendix K. The additions to Tables K3-1, K3-2, and K3-3 are provided in Attachment 4 to this ERD.

Appendix K, Section K3. As noted in the correction to the text for Section 7.3.1.1 above, the total number of epistemic parameters is 305 plus 87, or 392. This error also affects the text in Appendix K, Section K3. The corrected text for the second paragraph on Page K-6 is as follows:

*The vector **e** contains a total of nE = 392 elements. Thus, E is a subset of $R^{nE} = R^{392}$. However, not every element of **e** is used in uncertainty and sensitivity analysis for every scenario class. For example, **e** contains 44 elements corresponding to the dose conversion factors for inhalation pathways used to calculate the dose following an igneous eruptive event. These elements are only used in the igneous eruptive scenario class. In addition, certain of elements of **e** are correlated to other elements of **e**. Each subset of correlated variables is represented in the sensitivity analyses by one member of the set of correlated variables. By excluding variables that are not used in a scenario class and by choosing representatives for correlated sets of variables, the total number of uncertain input variables considered for the sensitivity analysis of a scenario class is less than 392, with the exact number depending on the scenario class.*

Figure 7.3.2-23. This figure title incorrectly refers to "Realization 2". The correct Figure title should read as follows:

Expected Annual Dose for 1,000,000 Years from Seismic Ground Motion for Aleatory Sample Size of 30 and 90

INTENTIONALLY LEFT BLANK

ATTACHMENT 1—CORRECTED TEXT FOR CR 11875:

7.7.3.3 Unsaturated Zone Flow

In the EPRI TSPA Analysis, the UZ flow above the repository is not represented by a process model as in the TSPA-LA Model, but is represented via lumped parameters incorporating time history of infiltration accounting for different climate states, flow focusing factor accounting for focused flow along fractures, and seepage into the repository. Infiltration rates for the different climate states used in the EPRI TSPA Analysis (Table M-1) compare reasonably well with the weighted mean infiltration rates used in the TSPA-LA Model (Table M-2). The seepage rates used in the EPRI TSPA Analysis (Table M-3a) are based on computed seepage and fraction of the repository experiencing flowing water summarized in *Abstraction of Drift Seepage* (CRWMS M&O 2001 [DIRS 154291], Table 16). A comparison of the seepage rates given in Table M-3a with those given in the recent analysis and/or model report (Table M-3b) indicates that when seepage occurs in the EPRI TSPA Analysis the seepage rates are higher than those in the TSPA-LA Model (Figure 7.7.3-1(a)). A comparison of the EPRI calculated base case seepage rates at high infiltration rates shows a good correlation between the seepage rates used in the TSPA-LA Model and the seepage rates used in the in EPRI TSPA Analysis (Figure 7.7.3-1(a)). For the high seepage case used in the EPRI TSPA Analysis, which has a small probability of occurrence (p=0.04, Table M-3a), the seepage rates are higher than those used in the TSPA-LA Model at comparable infiltration rates (Figure 7.7.3-1(a)). A comparison of the seepage fractions given in Table M-3a with those used in the TSPA-LA Model (Table M-3b) indicates that the seepage fractions used in the EPRI TSPA Analysis are lower than those in the TSPA-LA Model (Figure 7.7.3-1(b)), especially for the seepage used in the base case EPRI TSPA Analysis. Although the mean seepage rates in the EPRI TSPA Analysis are higher (when seepage occurs) than those in the TSPA-LA Model, a lower calculated seepage fraction results fewer waste packages potentially exposed to seepage water in the EPRI TSPA Analysis.

7.7.3.11 Mean Annual Dose Comparison—Nominal Case

The computed mean radionuclide doses for the EPRI nominal scenario is given on Figure 5-10 in Apted and Ross (2005 [DIRS 182229]). In comparison, the results from the TSPA-LA Model for the computed mean annual doses for the combined Nominal Scenario Modeling Case and the Waste Package EF Modeling Case are shown on Figure 7.7.3-3. The results indicate a similar pattern for the nominal scenario characterized by a significant increase in dose after 100,000 years. The early failure dose is represented by the dose increase after about 1,000 years in the TSPA-LA Model (Figure 7.7.3-3), which is somewhat delayed in the EPRI TSPA Analysis (Apted and Ross 2005 [DIRS 182229], Figure 5-10). The mean annual dose in the EPRI TSPA Analysis is about 2.0×10^{-2} mrem/yr compared to about 4.0×10^{-1} mrem/yr in the TSPA-LA Model after one-million years. The main contributor to mean annual dose at late time is ^{129}I in both cases.

The differences between the EPRI TSPA Analysis and the TSPA-LA Model results can be accounted for by differences in:

- Seepage fraction and seepage rates through the repository
- Early-failure representation and EBS failure curves
- Inventory, both in terms of waste type and individual radionuclides
- Solubility limits and sorption characteristics in the UZ and SZ
- Groundwater specific discharge in the SZ.

As shown in Figures 7.7.3-1(a) and 7.7.3-1(b), even though the seepage rates used in the EPRI TSPA Analysis are higher than the corresponding rates used in the TSPA-LA Model, the seepage fraction values are significantly smaller in the EPRI TSPA Analysis than in the TSPA-LA Model for the corresponding infiltration rates. The fewer number of packages that are subjected to seepage conditions causes a reduction in radionuclide release from the EBS, and contributes to the lower mean dose observed in the EPRI TSPA as compared to the TSPA-LA Model.

The EPRI TSPA Analysis only accounts for CSNF waste and considers failure of DS, WP, and cladding, whereas the TSPA-LA Model accounts for CSNF, DSNF, and HLW WPs, but does not take credit for cladding in CSNF WPs. Consequently, the overall dose release in the EPRI TSPA Analysis is delayed both during early failure case and for the nominal case. In addition, the EPRI TSPA Analysis uses a value of 0.37 m/yr for the groundwater specific discharge (Apted and Ross 2005 [DIRS 182229], Section 5.5.2.4.2), whereas the TSPA-LA Model uses a distribution of values ranging between 0.3 and 7.5 m/yr (SNL 2008 [183750], Table 6-6). The larger values of groundwater specific discharge used in the TSPA-LA Model contribute to earlier arrival of radionuclides in the groundwater, and hence to earlier observance of dose to the RMEI.

The EPRI TSPA Analysis only considers 12 radionuclides compared to 26 radionuclides in the TSPA-LA Model (Table M-4). During early failure ^{14}C is shown to contribute significantly to total dose in the TSPA-LA Model, which is not considered in the EPRI TSPA Analysis. At late time, the dominant radionuclides contributing to mean annual dose include ^{129}I, ^{99}Tc, ^{135}Cs, ^{79}Se, ^{242}Pu, and ^{237}Np in the TSPA-LA Model. The dominant radionuclides in the EPRI TSPA Analysis include ^{129}I followed by ^{237}Np, ^{233}U, and ^{235}U (Apted and Ross 2005 [DIRS 182229], Figure 5-10). However, the EPRI TSPA Analysis does not consider ^{135}Cs and ^{79}Se.

Solubility limits used in the EPRI TSPA Analysis indicate significantly lower values for neptunium, plutonium, and thorium compared to the range given in the TSPA-LA Model. On the other hand, sorption characteristics used in the EPRI TSPA Analysis for the UZ are significantly lower for uranium and plutonium compared to those in the TSPA-LA Model. However, this does not affect ^{129}I, ^{99}Tc, and ^{135}Cs, which represent the main contributors to mean annual dose in the TSPA-LA Model.

In general, the main features of the dose release curves for the nominal scenario compares reasonably well with the TSPA-LA Model. The differences can be related mostly to differences in seepage and in different implementation of the inventory and EBS failure characteristics. This is partly due to the fact that the EPRI TSPA Analysis uses earlier analysis and/or model report results.

Section 8 updates:

p. 8-43[a]. update first paragraph with the following:

The following estimates of mean net infiltration rate as a percentage of mean precipitation rate for each climate state are taken from Tables 6.5.7.1-3, 6.5.7.2-3, and 6.5.7.3-3 of the recent infiltration study (SNL 2008 [DIRS 182145]), namely:

- *Present-day climate:* $\overline{I} \sim$ *4.6% of* $\overline{P}$
- *Monsoon climate:* $\overline{I} \sim$ *6.2% of* $\overline{P}$
- Glacial-transition climate: $\overline{I} \sim$ 7.3% of $\overline{P}$

where $\overline{I}$ *is the mean net infiltration rate as a percentage of* $\overline{P}$ *, the mean precipitation rate. The mean net infiltration and precipitation rates for each climate state are generated by taking a weighted average of the spatially averaged rates for each of the four infiltration scenarios (defined by the 10th, 30th, 50th, and 90th percentiles of spatially averaged infiltration, see Section 6.3.1 of the parent document) presented in each table (Output DTN: MO0710PLOTSFIG.000 [DIRS 185207], file: Mean_Precip_Infil_Calcs.xls). The weighting factors (0.6191, 0.1568, 0.1645, and 0.0596) are based on a generalized likelihood uncertainty analysis described in Section 6.3.1.2 and Table 6.3.1-2 of the parent document, and they define the probability of occurrence of each of the four infiltration scenarios in the TSPA-LA Model. Ranges of net infiltration for the four infiltration scenarios can be summarized as follows. Estimated average present-day net infiltration ranges from less than 3 percent of precipitation for the drier 10th percentile infiltration scenario to about 13 percent of precipitation for the 90th percentile infiltration scenario (SNL 2008 [DIRS 182145], Table 6.5.7.1-3). For the monsoon climate, average net infiltration rate estimates for the 10th to 90th percentile infiltration scenarios range from about 3 percent to 17 percent of precipitation (SNL 2008 [DIRS 182145], Table 6.5.7.2-3). For the glacial-transition climate, the average net infiltration rate estimates for the 10th to 90th percentile infiltration scenarios range from about 5 percent to 16 percent of precipitation (SNL 2008 [DIRS 182145], Table 6.5.7.3-3). Note that the ratios of net infiltration to precipitation presented above are averaged over the entire infiltration model domain, not over the repository footprint area.*

p. 8-78[a]. replace 3rd and 4th line in Upper Natural Barrier first paragraph with the following.

(1) present-day climate: $\overline{I} \sim$ *4.6 percent of* $\overline{P}$*; (2) monsoon climate:* $\overline{I} \sim$ *6.2 percent of* $\overline{P}$*; and (3) glacial-transition climate:* $\overline{I} \sim$ *7.3 percent of* $\overline{P}$.

ATTACHMENT 2—APPENDIX K FIGURE UPDATE

(a)

	3,000 years			5,000 years			10,000 years		
Step[a]	Variable[b]	R^2[c]	SRRC[d]	Variable	R^2	SRRC	Variable	R^2	SRRC
1	INFIL	0.18	0.45	INFIL	0.19	0.44	MICTC99	0.15	0.36
2	MICTC99	0.31	0.32	MICTC99	0.32	0.34	INFIL	0.27	0.35
3	SZGWSPDM	0.40	0.31	SEEPPRM	0.42	-0.31	SZGWSPDM	0.37	0.33
4	SEEPPRM	0.49	-0.29	SZGWSPDM	0.49	0.29	DTDRHUNC	0.45	0.26
5	SEEPUNC	0.57	0.30	SEEPUNC	0.57	0.31	SEEPPRM	0.49	-0.16
6	CSSPECSA	0.62	0.22	CSSPECSA	0.62	0.21	SZCOLRAL	0.52	-0.19
7	SZFISPVO	0.66	0.22	SZFISPVO	0.65	0.18	SZFISPVO	0.55	0.18
8	CSNFMASS	0.68	0.15	ALPHAL	0.67	-0.16	SZFIPOVO	0.56	-0.14
9	MICC14	0.69	0.14	CSNFMASS	0.68	0.18	CSNFMASS	0.58	0.13
10	SZDIFCVO	0.71	-0.14	MICC14	0.70	0.12	SZDIFCVO	0.59	-0.13
11	ALPHAL	0.73	-0.14	SZCOLRAL	0.71	-0.14	MICAM243	0.61	0.13
12	MICSE79	0.74	0.09	SZFIPOVO	0.72	-0.12	CSSPECSA	0.62	0.13
13	SZFIPOVO	0.74	-0.10	SZCOLRVO	0.73	-0.12	CSWFA4AC	0.63	0.12
14	SZCOLRVO	0.75	-0.08	MICSN126	0.74	0.10	KDUSMEC	0.64	0.11
15	THERMCON	0.76	-0.08	SZDIFCVO	0.75	-0.10			
16				CSWFA4AC	0.76	0.09			

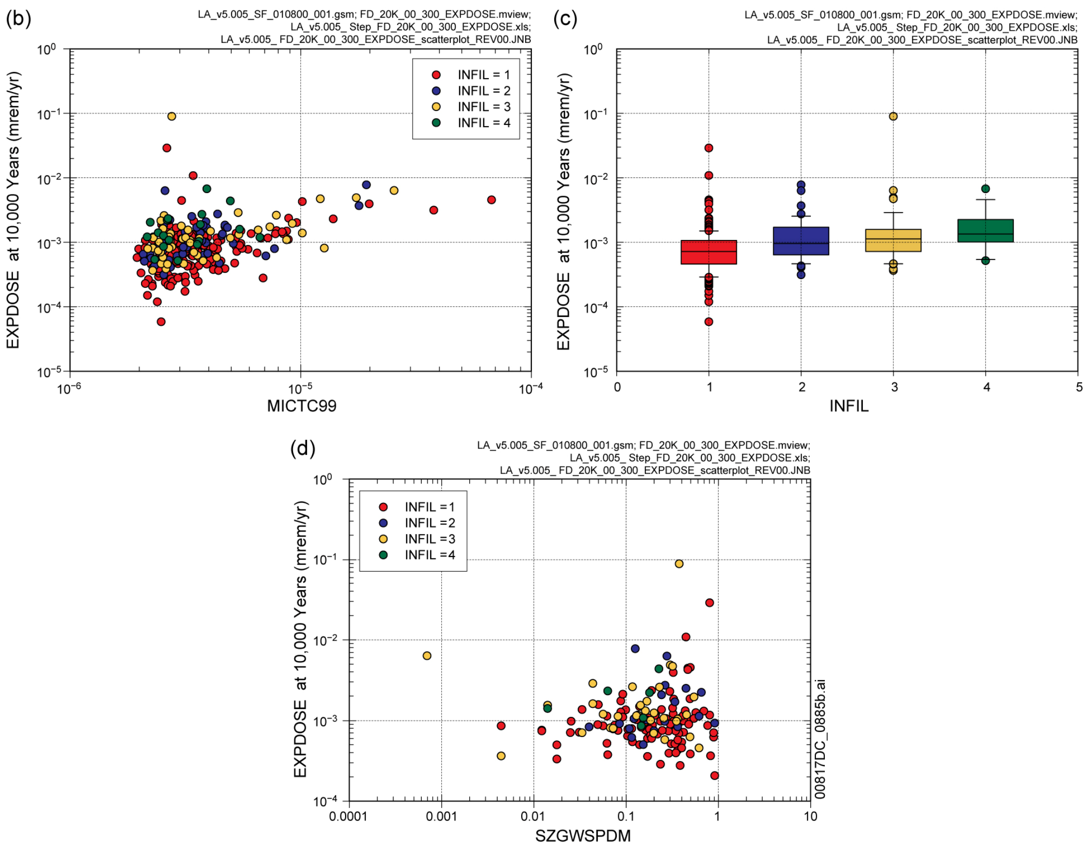

Source: Output DTNs: MO0710ADTSPAWO.000 [DIRS 183752]; and MO0710PLOTSFIG.000 [DIRS 185207].

NOTE: In (c), the box extends from 0.25 to 0.75 quantile; lower and upper bar and whisker extend to 0.1 and 0.9 quantile, respectively; dots represent values outside 0.1 to 0.9 quantile range; median indicated by light horizontal line.

Figure K7.8.1-2[a]. Stepwise rank regression analyses and selected scatterplots for expected dose to RMEI (*EXPDOSE*, mrem/yr) over [0, 20,000 yr] for all radioactive species resulting from seismic fault displacement: (a) regressions for *EXPDOSE* at 3,000, 5,000, and 10,000 years, and (b,c,d) scatterplots for *EXPDOSE* at 10,000 years

(a)

	50,000 years			200,000 years			500,000 years		
Step[a]	Variable[b]	R^2[c]	SRRC[d]	Variable	R^2	SRRC	Variable	R^2	SRRC
1	SZGWSPDM	0.25	0.51	INFIL	0.15	0.37	INFIL	0.18	0.40
2	INFIL	0.37	0.31	SZGWSPDM	0.29	0.40	EP1LOWPU	0.29	0.33
3	WPFLUX	0.43	0.22	WPFLUX	0.37	0.28	SZGWSPDM	0.38	0.36
4	EP1LOWPU	0.48	0.21	EP1LOWPU	0.44	0.28	WPFLUX	0.43	0.25
5	SEEPPRM	0.52	−0.19	SEEPPRM	0.48	−0.22	GOESITED	0.48	−0.18
6	MICNP237	0.55	0.18	SZFISPVO	0.55	0.19	SEEPPRM	0.52	−0.20
7	CPUCOLWF	0.57	0.17	SEEPUNC	0.57	0.17	MICPU239	0.54	0.19
8	SZCOLRAL	0.60	−0.15	CORRATSS	0.59	−0.10	SEEPUNC	0.57	0.17
9	SZFISPVO	0.62	0.16	EP1NPO2	0.60	0.11	SZFISPVO	0.60	0.17
10	SEEPUNC	0.63	0.12	SZCONCOL	0.62	0.11	SZCONCOL	0.62	0.14
11	PHCSS	0.65	−0.12	EP1LOWNU	0.63	0.12	EP1LOWNU	0.64	0.18
12	HFOSA	0.66	−0.11	SZDIFCVO	0.64	−0.11	UZFAG4	0.67	−0.15
13	RUBMAXL	0.67	−0.10	SZKDAMCO	0.65	0.10	HFOSA	0.68	−0.11
14	PH2MCONS	0.67	−0.09	GOESITED	0.66	−0.11	SZDIFCVO	0.69	−0.12
15				MICPU239	0.67	0.19	KDPUSMEC	0.70	0.10
16				UZFAG4	0.68	−0.11	SZWBNDAL	0.71	−0.10

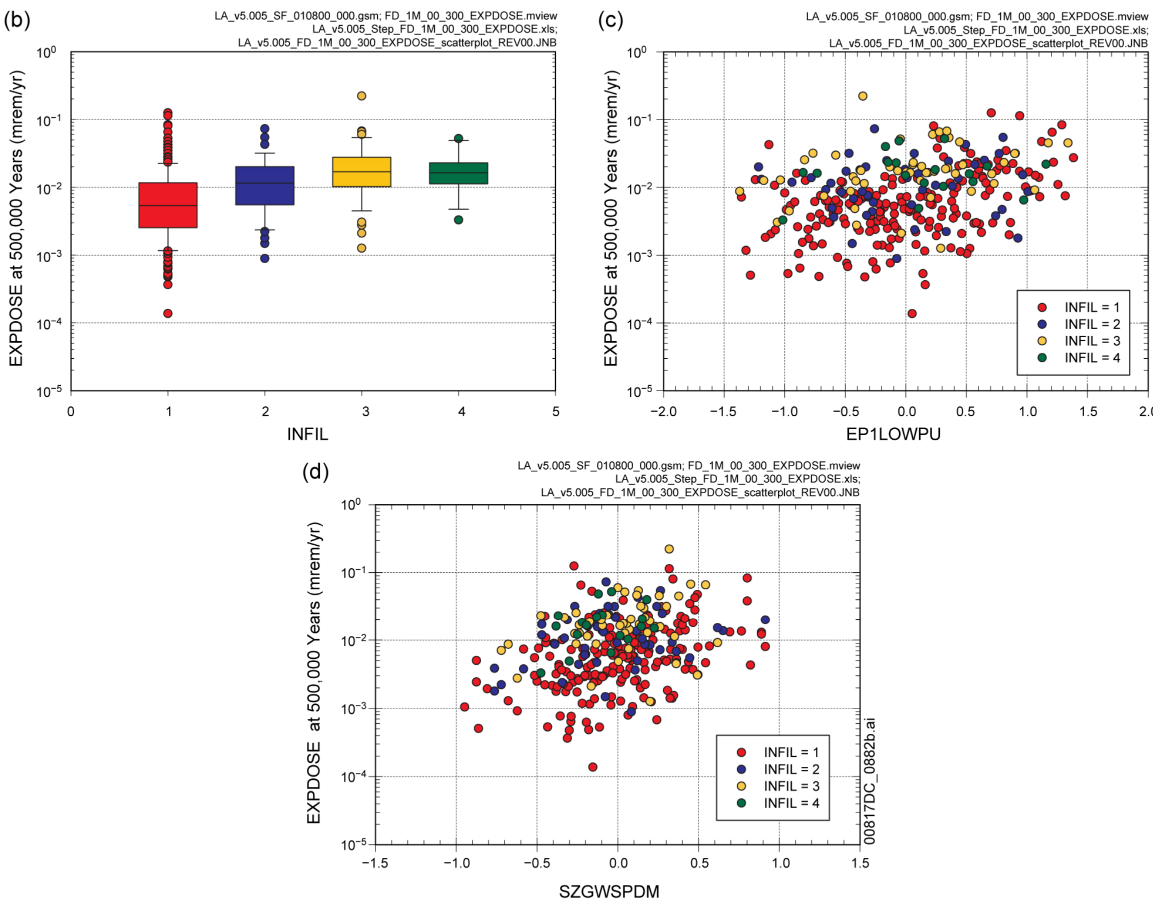

Source: Output DTNs: MO0710ADTSPAWO.000 [DIRS 183752]; and MO0710PLOTSFIG.000 [DIRS 185207].

NOTE: In (c), the box extends from 0.25 to 0.75 quantile; lower and upper bar and whisker extend to 0.1 and 0.9 quantile, respectively; dots represent values outside 0.1 to 0.9 quantile range; median indicated by light horizontal line.

Figure K7.8.2-2[a]. Stepwise rank regression analyses and selected scatterplots for expected dose to RMEI (*EXPDOSE*, mrem/yr) over [0, 1,000,000 yr] for all radioactive species resulting from seismic fault displacement: (a) regressions for *EXPDOSE* at 50,000, 200,000, and 500,000 years, and (b,c,d) scatterplots for *EXPDOSE* at 500,000 years

ATTACHMENT 3—APPENDIX J FONT UPDATE

The pages with symbol changes are as follows.

Character	Page Number	Number of Occurrences
S	J-22	14
A	J-24	2
	J-27	1
	J-28	2
	J-30	6
	J-32	2
	J-33	3
	J-39	3
	J-46	4
	J-47	1
	J-48	3
	J-52	1
E	J-25	2
	J-36	1
	J-38	3
	J-39	5
	J-41	1
	J-48	3
	J-49	1
	J-67	1

ATTACHMENT 4

Additional Corrections to Appendix K Tables

The corrections to the Appendix K Tables do not require any changes to references currently listed in the Volume III DIRS report. However, the additions to Table K3-3 did require some new input values to be added to a reference already listed on the Volume III DIRS report.

Add to Table K3-1

MICPU242*. Groundwater Biosphere Dose Conversion Factor (BDCF) for ^{242}Pu in modern interglacial climate ((Sv/year)/(Bq/m^3)). *Distribution:* Discrete. *Range:* 3.31E-07 to 2.79E-06. *Mean:* 9.07E-07. *Standard Deviation:* 3.20E-07. *TSPA-LA Name:* GW_BDCF_MIC_Pu242. *Location in TSPA-LA:* Sections 6.3.11.2 and 6.3.11.3; Table 6.3.11-3.
MICRA228*. Groundwater Biosphere Dose Conversion Factor (BDCF) for ^{228}Ra in modern interglacial climate ((Sv/year)/(Bq/m^3)). *Distribution:* Discrete. *Range:* 6.14E-07 to 1.53E-06. *Mean:* 9.05E-07. *Standard Deviation:* 1.40E-07. *TSPA-LA Name:* GW_BDCF_MIC_Ra228. *Location in TSPA-LA:* Sections 6.3.11.2 and 6.3.11.3; Table 6.3.11-3.
MICTH230*. Groundwater Biosphere Dose Conversion Factor (BDCF) for ^{230}Th in modern interglacial climate ((Sv/year)/(Bq/m^3)). *Distribution:* Discrete. *Range:* 2.74E-07 to 3.27E-06. *Mean:* 1.08E-06. *Standard Deviation:* 4.34E-07. *TSPA-LA Name:* GW_BDCF_MIC_Th230. *Location in TSPA-LA:* Sections 6.3.11.2 and 6.3.11.3; Table 6.3.11-3.
MICTH232*. Groundwater Biosphere Dose Conversion Factor (BDCF) for ^{232}Th in modern interglacial climate ((Sv/year)/(Bq/m^3)). *Distribution:* Discrete. *Range:* 5.05E-07 to 5.26E-06. *Mean:* 1.85E-06. *Standard Deviation:* 7.33E-07. *TSPA-LA Name:* GW_BDCF_MIC_Th232. *Location in TSPA-LA:* Sections 6.3.11.2 and 6.3.11.3; Table 6.3.11-3.
MICU235*. Groundwater Biosphere Dose Conversion Factor (BDCF) for ^{235}U in modern interglacial climate ((Sv/year)/(Bq/m^3)). *Distribution:* Discrete. *Range:* 3.91E-08 to 2.97E-07. *Mean:* 9.41E-08. *Standard Deviation:* 3.67E-08. *TSPA-LA Name:* GW_BDCF_MIC_U235. *Location in TSPA-LA:* Sections 6.3.11.2 and 6.3.11.3; Table 6.3.11-3.
MICU236*. Groundwater Biosphere Dose Conversion Factor (BDCF) for ^{236}U in modern interglacial climate ((Sv/year)/(Bq/m^3)). *Distribution:* Discrete. *Range:* 3.75E-08 to 2.02E-07. *Mean:* 7.67E-08. *Standard Deviation:* 2.60E-08. *TSPA-LA Name:* GW_BDCF_MIC_U236. *Location in TSPA-LA:* Sections 6.3.11.2 and 6.3.11.3; Table 6.3.11-3.

Replacements for existing entries in Table K3-1

FRACCHNL. Fraction of the RMEI location subject to fluvial deposition (dimensionless). *Distribution:* Uniform. *Range:* 0.09 to 0.54. *TSPA-LA Name:* Fraction_Channel_a. *Location in TSPA-LA:* Table 6.5-5.
RHI85. The in-drift precipitated/salts (IDPS) process model uncertainty factor for the logarithm of the ionic strength of the in-drift waters at high relative humidity (≥85%) (log molal). *Distribution:* Triangular. *Range:* -0.1 to 0.1. *Mean/Median/Mode:* 0. *TSPA-LA Name:* PCE_I_Uncert_RH_85_100_a. *Location in TSPA-LA:* Section 6.3.4.1; Table 6.3.4-3.
SEEPCOND. Pointer variable to determine the seepage/condensation regime for the first failed waste package in a percolation subregion (dimensionless). *Distribution:* Uniform. *Range:* 0 to 1. *TSPA-LA Name:* Seepage_Condensation_Prob_a. *Location in TSPA-LA:* Section 6.3.3.2.2; Table 6.3.3-5.
WDDSAGGC. Topside general corrosion rate of the drip shield (nm/yr). *Distribution:* Student-t with 5 degrees of freedom. *Mean:* 46.1. *Standard Deviation:* 1.19. *TSPA-LA Name:* WDDSAggrGC_Mean_a. *Location in TSPA-LA:* Sections 6.3.5.1.2 and 6.3.5.1.3; Table 6.3.5-3.

Add to Table K3-2

GW_BDCF_MIC_Pu242*. Groundwater Biosphere Dose Conversion Factor (BDCF) for ^{242}Pu in modern interglacial climate ((Sv/year)/(Bq/m^3)). *Distribution:* Discrete. *Range:* 3.31E-07 to 2.79E-06. *Mean:* 9.07E-07. *Standard Deviation:* 3.20E-07. *Sensitivity Name:* MICPU242. *Location in TSPA-LA:* Sections 6.3.11.2 and 6.3.11.3; Table 6.3.11-3.

GW_BDCF_MIC_Ra228*. Groundwater Biosphere Dose Conversion Factor (BDCF) for ^{228}Ra in modern interglacial climate ((Sv/year)/(Bq/m^3)). *Distribution:* Discrete. *Range:* 6.14E-07 to 1.53E-06. *Mean:* 9.05E-07. *Standard Deviation:* 1.40E-07. *Sensitivity Name:* MICRA228. *Location in TSPA-LA:* Sections 6.3.11.2 and 6.3.11.3; Table 6.3.11-3.
GW_BDCF_MIC_Th230*. Groundwater Biosphere Dose Conversion Factor (BDCF) for ^{230}Th in modern interglacial climate ((Sv/year)/(Bq/m^3)). *Distribution:* Discrete. *Range:* 2.74E-07 to 3.27E-06. *Mean:* 1.08E-06. *Standard Deviation:* 4.34E-07. *Sensitivity Name:* MICTH230. *Location in TSPA-LA:* Sections 6.3.11.2 and 6.3.11.3; Table 6.3.11-3.
GW_BDCF_MIC_Th232*. Groundwater Biosphere Dose Conversion Factor (BDCF) for ^{232}Th in modern interglacial climate ((Sv/year)/(Bq/m^3)). *Distribution:* Discrete. *Range:* 5.05E-07 to 5.26E-06. *Mean:* 1.85E-06. *Standard Deviation:* 7.33E-07. *Sensitivity Name:* MICTH232. *Location in TSPA-LA:* Sections 6.3.11.2 and 6.3.11.3; Table 6.3.11-3.
GW_BDCF_MIC_U235*. Groundwater Biosphere Dose Conversion Factor (BDCF) for ^{235}U in modern interglacial climate ((Sv/year)/(Bq/m^3)). *Distribution:* Discrete. *Range:* 3.91E-08 to 2.97E-07. *Mean:* 9.41E-08. *Standard Deviation:* 3.67E-08. *Sensitivity Name:* MICU235. *Location in TSPA-LA:* Sections 6.3.11.2 and 6.3.11.3; Table 6.3.11-3.
GW_BDCF_MIC_U236*. Groundwater Biosphere Dose Conversion Factor (BDCF) for ^{236}U in modern interglacial climate ((Sv/year)/(Bq/m^3)). *Distribution:* Discrete. *Range:* 3.75E-08 to 2.02E-07. *Mean:* 7.67E-08. *Standard Deviation:* 2.60E-08. *Sensitivity Name:* MICU236. *Location in TSPA-LA:* Sections 6.3.11.2 and 6.3.11.3; Table 6.3.11-3.

<u>Replacements for existing entries in Table K3-2</u>

Fraction_Channel_a - Fraction of the RMEI location subject to fluvial deposition (dimensionless). *Distribution:* Uniform. *Range:* 0.09 to 0.54. *Sensitivity Name:* FRACCHNL. *Location in TSPA-LA:* Table 6.5-5.
PCE_I_Uncert_RH_85_100_a - The IDPS process model uncertainty factor for the logarithm of the ionic strength of the in-drift waters at high relative humidity (≥85%) (log molal). *Distribution:* Triangular. *Range:* -0.1 to 0.1. *Mean/Median/Mode:* 0. *Sensitivity Name:* RHI85. *Location in TSPA-LA:* Section 6.3.4.1; Table 6.3.4-3.
Seepage_Condensation_Prob_a - Pointer variable to determine the seepage/condensation regime for the first failed waste package in a percolation subregion (dimensionless). *Distribution:* Uniform. *Range:* 0 to 1. *Sensitivity Name:* SEEPCOND. *Location in TSPA-LA:* Section 6.3.3.2.2; Table 6.3.3-5.
WDDSAggrGC_Mean_a - Topside general corrosion rate of the drip shield (nm/yr). *Distribution:* Student-t with 5 degrees of freedom. *Mean:* 46.1. *Standard Deviation:* 1.19. *Sensitivity Name:* WDDSAGGC. *Location in TSPA-LA:* Sections 6.3.5.1.2 and 6.3.5.1.3; Table 6.3.5-3.

<u>Add to Table K3-3</u>

GW_BDCF_MIC_Pu242*. Groundwater Biosphere Dose Conversion Factor (BDCF) for ^{242}Pu in modern interglacial climate ((Sv/year)/(Bq/m^3)). *Distribution:* Discrete. *Range:* 3.31E-07 to 2.79E-06. *Mean:* 9.07E-07. *Standard Deviation:* 3.20E-07. *Additional Information:* See GW_BDCF_MIC_Ac227. *Sensitivity Name:* MICPU242. *Location in TSPA-LA:* Sections 6.3.11.2 and 6.3.11.3; Table 6.3.11-3. *DTN:* MO0702PAGBDCFS.001_R0 [DIRS 179327]. *References:* *Biosphere Model Report* (SNL 2007 [DIRS 177399], Sections 1, 6.1, 6.4, 6.4.10, 6.8.10, 6.11 and 6.13; Equations 6.4.10-2, 6.4.10-4, 6.2.10-5 and 6.11-5; Tables 6.11-8 and 6.11-12).
GW_BDCF_MIC_Ra228*. Groundwater Biosphere Dose Conversion Factor (BDCF) for ^{228}Ra in modern interglacial climate ((Sv/year)/(Bq/m^3)). *Distribution:* Discrete. *Range:* 6.14E-07 to 1.53E-06. *Mean:* 9.05E-07. *Standard Deviation:* 1.40E-07. *Additional Information:* See GW_BDCF_MIC_Ac227. *Sensitivity Name:* MICTH228. *Location in TSPA-LA:* Sections 6.3.11.2 and 6.3.11.3; Table 6.3.11-3. *DTN:* MO0702PAGBDCFS.001_R0 [DIRS 179327]. *References:* *Biosphere Model Report* (MDL-MGR-MD-000001 REV 02, SNL 2007 [DIRS 177399], Sections 1, 6.1, 6.4, 6.4.10, 6.8.10, 6.11 and 6.13; Equations 6.4.10-2, 6.4.10-4, 6.2.10-5 and 6.11-5; Tables 6.11-8 and 6.11-12).

GW_BDCF_MIC_Th230*. Groundwater Biosphere Dose Conversion Factor (BDCF) for ^{230}Th in modern interglacial climate ((Sv/year)/(Bq/m^3)). *Distribution:* Discrete. *Range:* 2.74E-07 to 3.27E-06. *Mean:* 1.08E-06. *Standard Deviation:* 4.34E-07. *Additional Information:* See GW_BDCF_MIC_Ac227. *Sensitivity Name:* MICTH230. *Location in TSPA-LA:* Sections 6.3.11.2 and 6.3.11.3; Table 6.3.11-3. *DTN:* MO0702PAGBDCFS.001_R0 [DIRS 179327]. *References: Biosphere Model Report* (MDL-MGR-MD-000001 REV 02, SNL 2007 [DIRS 177399], Sections 1, 6.1, 6.4, 6.4.10, 6.8.10, 6.11 and 6.13; Equations 6.4.10-2, 6.4.10-4, 6.2.10-5 and 6.11-5; Tables 6.11-8 and 6.11-12).
GW_BDCF_MIC_Th232*. Groundwater Biosphere Dose Conversion Factor (BDCF) for ^{232}Th in modern interglacial climate ((Sv/year)/(Bq/m^3)). *Distribution:* Discrete. *Range:* 5.05E-07 to 5.26E-06. *Mean:* 1.85E-06. *Standard Deviation:* 7.33E-07. *Additional Information:* See GW_BDCF_MIC_Ac227. *Sensitivity Name:* MICTH232. *Location in TSPA-LA:* Sections 6.3.11.2 and 6.3.11.3; Table 6.3.11-3. *DTN:* MO0702PAGBDCFS.001_R0 [DIRS 179327]. *References: Biosphere Model Report* (MDL-MGR-MD-000001 REV 02, SNL 2007 [DIRS 177399], Sections 1, 6.1, 6.4, 6.4.10, 6.8.10, 6.11 and 6.13; Equations 6.4.10-2, 6.4.10-4, 6.2.10-5 and 6.11-5; Tables 6.11-8 and 6.11-12).
GW_BDCF_MIC_U235*. Groundwater Biosphere Dose Conversion Factor (BDCF) for ^{235}U in modern interglacial climate ((Sv/year)/(Bq/m^3)). *Distribution:* Discrete. *Range:* 3.91E-08 to 2.97E-07. *Mean:* 9.41E-08. *Standard Deviation:* 3.67E-08. *Additional Information:* See GW_BDCF_MIC_Ac227. *Sensitivity Name:* MICU235. *Location in TSPA-LA:* Sections 6.3.11.2 and 6.3.11.3; Table 6.3.11-3. *DTN:* MO0702PAGBDCFS.001_R0 [DIRS 179327]. *References: Biosphere Model Report* (SNL 2007 [DIRS 177399], Sections 1, 6.1, 6.4, 6.4.10, 6.8.10, 6.11 and 6.13; Equations 6.4.10-2, 6.4.10-4, 6.2.10-5 and 6.11-5; Tables 6.11-8 and 6.11-12).
GW_BDCF_MIC_U236*. Groundwater Biosphere Dose Conversion Factor (BDCF) for ^{236}U in modern interglacial climate ((Sv/year)/(Bq/m^3)). *Distribution:* Discrete. *Range:* 3.75E-08 to 2.02E-07. *Mean:* 7.67E-08. *Standard Deviation:* 2.60E-08. *Additional Information:* See GW_BDCF_MIC_Ac227. *Sensitivity Name:* MICU236. *Location in TSPA-LA:* Sections 6.3.11.2 and 6.3.11.3; Table 6.3.11-3. *DTN:* MO0702PAGBDCFS.001_R0 [DIRS 179327]. *References: Biosphere Model Report* (SNL 2007 [DIRS 177399], Sections 1, 6.1, 6.4, 6.4.10, 6.8.10, 6.11 and 6.13; Equations 6.4.10-2, 6.4.10-4, 6.2.10-5 and 6.11-5; Tables 6.11-8 and 6.11-12).

Replacements for existing entries in Table K3-3

PCE_I_Uncert_RH_85_100_a. The IDPS process model uncertainty factor for the logarithm of the ionic strength of the in-drift waters at high relative humidity (≥85%) (log molal). *Distribution:* Triangular. *Range:* -0.1 to 0.1. *Mean/Median/Mode:* 0. *Additional Information:* IDPS uncertainty factors for the Cl, N, Cl:N, and I of in-drift water are used directly by the Physical and Chemical Environment (P&CE) abstraction models. Four values are extracted from the seepage evaporation/dilution lookup tables. No uncertainty is associated with the ionic strength below 85 percent relative humidity from the lookup tables because the ionic strength is not used by TSPA at these concentrations. Between 85 percent and 100 percent relative humidity the ionic strength is adjusted for uncertainty by applying a triangular distribution. Between 100 and 95 percent relative humidity in the drift, the ionic strength of the evaporating solutions exceeds 1 molal. At the lower relative humidity conditions, concentrations of well over 10 molal are possible. The key chemical parameters that are provided to TSPA-LA by the P&CE dilution/evaporation abstraction model are pH, ionic strength, Cl^- and NO_3^- as a function of relative humidity. *Sensitivity Name:* RHI85. *Location in TSPA-LA:* Section 6.3.4.1; Table 6.3.4-3. *DTN:* SN0703PAEBSPCE.007_R2 [DIRS 184141]. *References: Engineered Barrier System: Physical and Chemical Environment* (SNL 2007 [DIRS 177412], Sections 4.1.17.1, 6.2.1.1.2, 6.12.3 and 6.13.3; Tables 4.1-10, 6.9-1 and 6.12-1; Equation 6.2-8).
Seepage_Condensation_Prob_a. Pointer variable to determine the seepage/condensation regime for the first failed waste package in a percolation subregion (dimensionless). *Distribution:* Uniform. *Range:* 0 to 1. *Additional Information:* Parameter determined within TSPA. *Sensitivity Name:* SEEPCOND. *Output DTN:* MO0708TSPAGENT.000_R0 [DIRS 183000]. *Location in TSPA-LA:* Section 6.3.3.2.2; Table 6.3.3-5.

WDDSAggrGC_Mean_a. Topside general corrosion rate of the drip shield (nm/yr). *Distribution:* Student-t with 5 degrees of freedom. *Mean:* 46.1. *Standard Deviation:* 1.19. *Additional Information:* The corrosion of the underside surface of the drip shield is more likely to be dry oxidation and humid-air corrosion, while the topside surface of the drip shield is more likely to undergo dry oxidation, humid-air and aqueous-phase corrosion. The topside surfaces that are subject to seepage dripping may be exposed to more aggressive chemical environment and conditions than those not subject to seepage dripping. The underside surfaces, where seepage cannot physically contact and dust cannot settle and accumulate, are not expected to be exposed to seepage water, and therefore corrosion will proceed under benign conditions. For the modeling purpose, the entire variation in the data is assumed to be due to the variability in the corrosion process. The resulting normal probability model represents the variability in the drip shield general corrosion rates for the aggressive conditions. The variability in the general corrosion rate is likely due to the randomness of the corrosion process under the conditions in the exposure environment. Recorded in the TSPA Input Database as two constants: WDDSAggrGC_Uncert_Mean and WDDSAggrGC_Uncert_SD. *Sensitivity Name:* WDDSAGGC. *Location in TSPA-LA:* Sections 6.3.5.1.2 and 6.3.5.1.3; Table 6.3.5-3. *DTN:* SN0704PADSGCMT.001_R2 [DIRS 182122]. *References: General Corrosion and Localized Corrosion of the Drip Shield* (SNL 2007 [DIRS 180778], Sections 1.3[a], 6.1.6.2[a] and 8.1[a]; Table 8-1[a]).

ATTACHMENT 5—SUPPLEMENTAL PLOTS

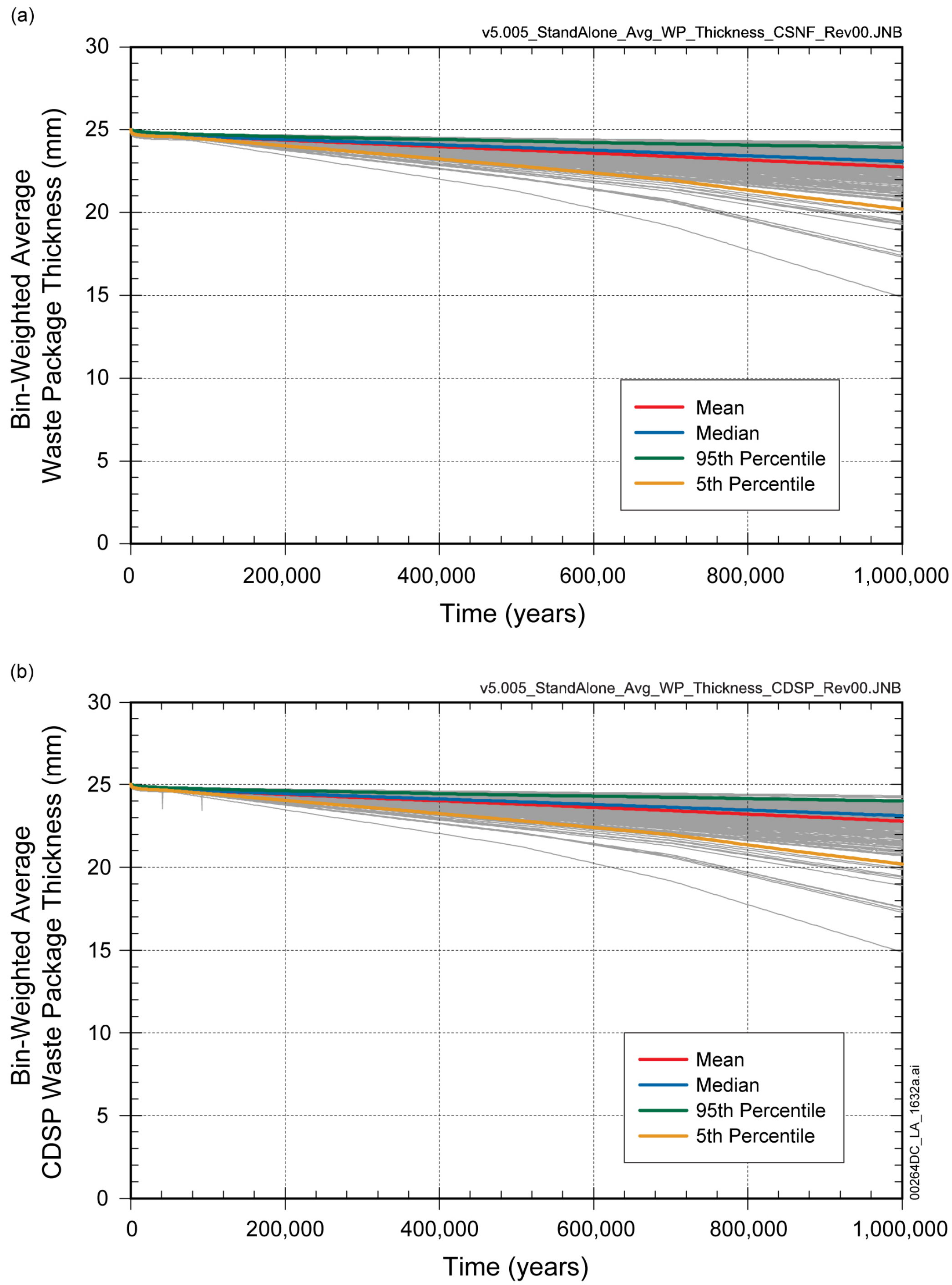

Source: Output DTN: MO0803TSPAPSAR.000 [DIRS 185276]

NOTE: These plots show epistemic uncertainty in average waste package thickness, where "average thickness" represents a triple average over (1) all patches on a individual waste package, (2) all waste packages in a percolation subregion or "bin", and (3) all percolation subregions.

Figure 7.3.2-15[a]. Spatially Averaged Waste Package Outer Barrier Thickness for 1 Million Years for (a) CSNF Waste Packages and (b) CDSP Waste Packages

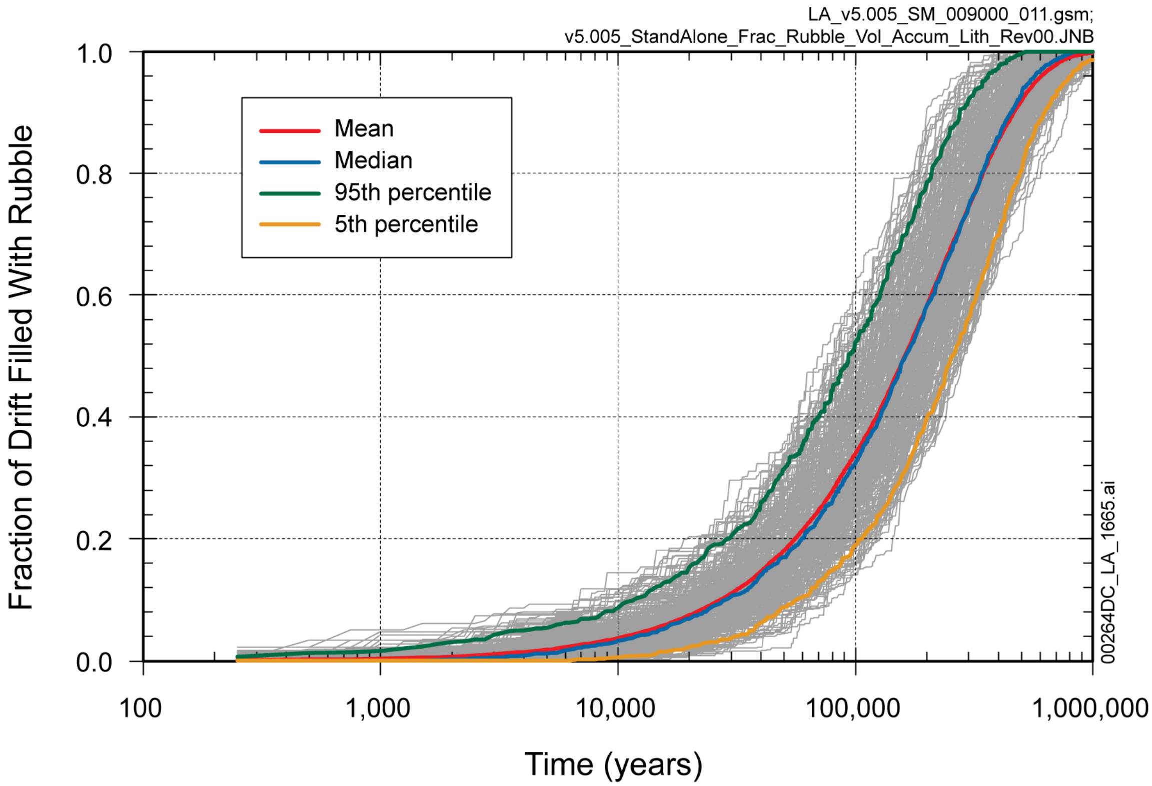

Source: Output DTN: MO0803TSPAPSAR.000 [DIRS 185276].

NOTE: Volume of rubble per meter of drift that is required to fill the drift is sampled for each epistemic realization and ranges uniformly between 30 m^3/m to 120 m^3/m.

Figure 8.3-7c[a]. Fraction of Drift Filled with Rubble

INTENTIONALLY LEFT BLANK